Supplement of Atmos. Chem. Phys., 23, 6703–6718, 2023
https://doi.org/10.5194/acp-23-6703-2023-supplement

Atmospheric Chemistry and Physics Open Access

Supplement of

Measurement of the collision rate coefficients between atmospheric ions and multiply charged aerosol particles in the CERN CLOUD chamber

Joschka Pfeifer et al.

Correspondence to: Joschka Pfeifer (joschka.pfeifer@cern.ch)

S1 Sulfuric acid measurements

Figure S1 shows the sulfuric acid concentration measured during the experiments. The gas phase concentration was measured using a Nitrate CI-APi-TOF (Kürten et al., 2011). Our rate coefficients in the main text were obtained during decay stages. In Figure S1, we note that under the experimental conditions (278 K at 80 % relative humidity), nucleation, and vapor condensation can be neglected during these stages (Vehkamäki et al., 2002; Nieminen et al., 2010; Dunne et al., 2016). As an example, for sulfuric acid concentrations of 5×10^7 cm^{-3}, condensation growth rates are below 2 nm hour^{-1} and the nucleation rate is below 1×10^{-2} cm^{-3} s^{-1} (Dunne et al., 2016). Moreover, while these values are already small compared to the observed time scale of the rate coefficients of multiply charged particles, sulfuric acid concentrations of ~5×10^7 cm^{-3} are only measured at the beginning of a decay stage and quickly drop well below 1×10^7 cm^{-3}. Figure S1 also shows that gas phase sulfuric acid concentration is comparable during both multiply charged experiments (LHS) and Steady State experiments (RHS).

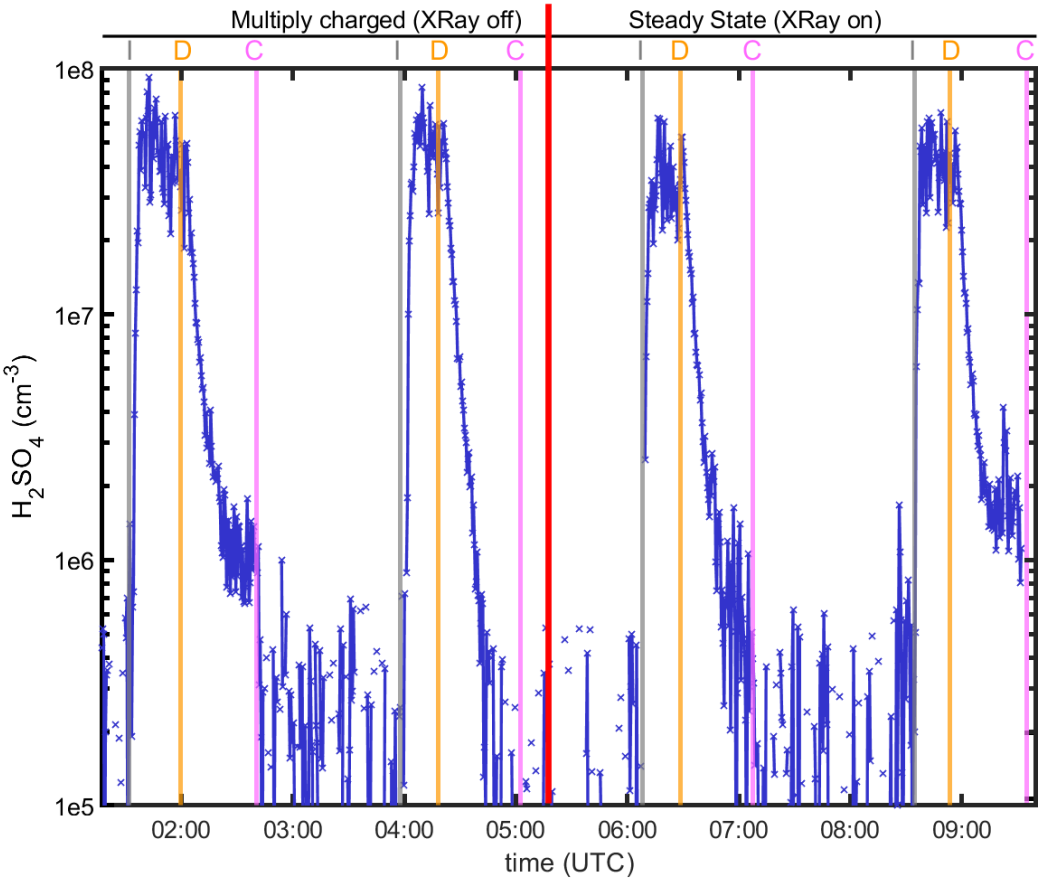

Figure S1: Measured Sulfuric Acid concentration during the experiments. The letters I, D and C show the transition from "Injection" (I) to "Decay" (D) to "Cleaning" (C) stage.

S2 Validation of inferred rate coefficients

The resultant error in calculating the ion–aerosol rate coefficients consists of statistical and systematic errors. We verify the robustness of our calculations by varying parameters and constants within ranges of uncertainty (Figure S2). We repeat our numerical calculations (Eq. 5–9) for each experiment 1000 times by varying all parameters that contribute to systematic errors in our inference. During these calculations, the parameters are drawn from a normal distribution around the used values.

In Eq. (4) (main text), the inferred multiply charged distribution ω_j depends on assumed maximum number of charges j, the loss timescale coefficient k_{loss}, and the baseline distribution $\Omega_+(t=0)$. In our uncertainty estimate, we allow the maximum j to vary between 6 and 15 charges. The loss timescale $k(d_{\mathrm{p}}, t)$ is allowed to vary by ± 500% to account for neglected loss rates and for possible errors in the particle measurements. Additionally, we allow variation of ± 50 % of the baseline distribution atop of its value and ±10 % below. We set the statistical error on the measured NAIS current to be in the range of ± 0.2 fA (which is an uncertainty obtained from chamber background measurements). This value is randomly varied prior to inversion.

The systematic error of the nSMPS instrument (coupled with a condensation particle counter 2.5 nm, CPC 2.5) is large for the size range of our experiments (about 70 %) (Kangasluoma et al., 2020). We see this uncertainty confirmed for our experiments in comparison with another Condensation Particle Counter (CPC 2.5), which is why we treat the SMPS instrument with a 400 % uncertainty. This rather large uncertainty does not affect the conclusion from our calculations because wall and dilution losses clearly dominate loss rates of the affected particles (Figure 2, main text). During these calculations, we also allow the particle density to vary between pure water (998 kg m^{-3}) and pure sulfuric acid (1830 kg m^{-3}). An example of the procedure for the allowed number of charged and for particle density is shown in Figure S2. The figure also shows the weighting scheme applied to the calculated coefficients.

In Table S1, we summarize the allowed uncertainty for all parameters during the procedure shown in Figure S2. Figure S3 shows the ± 1 standard deviation range of these calculations and compares it with the coefficients shown in Figure 4 (main text). The variations confirm the robustness of our calculated rate coefficients and even a drastic variation of the initial assumptions and an allowance for large instrumental errors confirms our results.

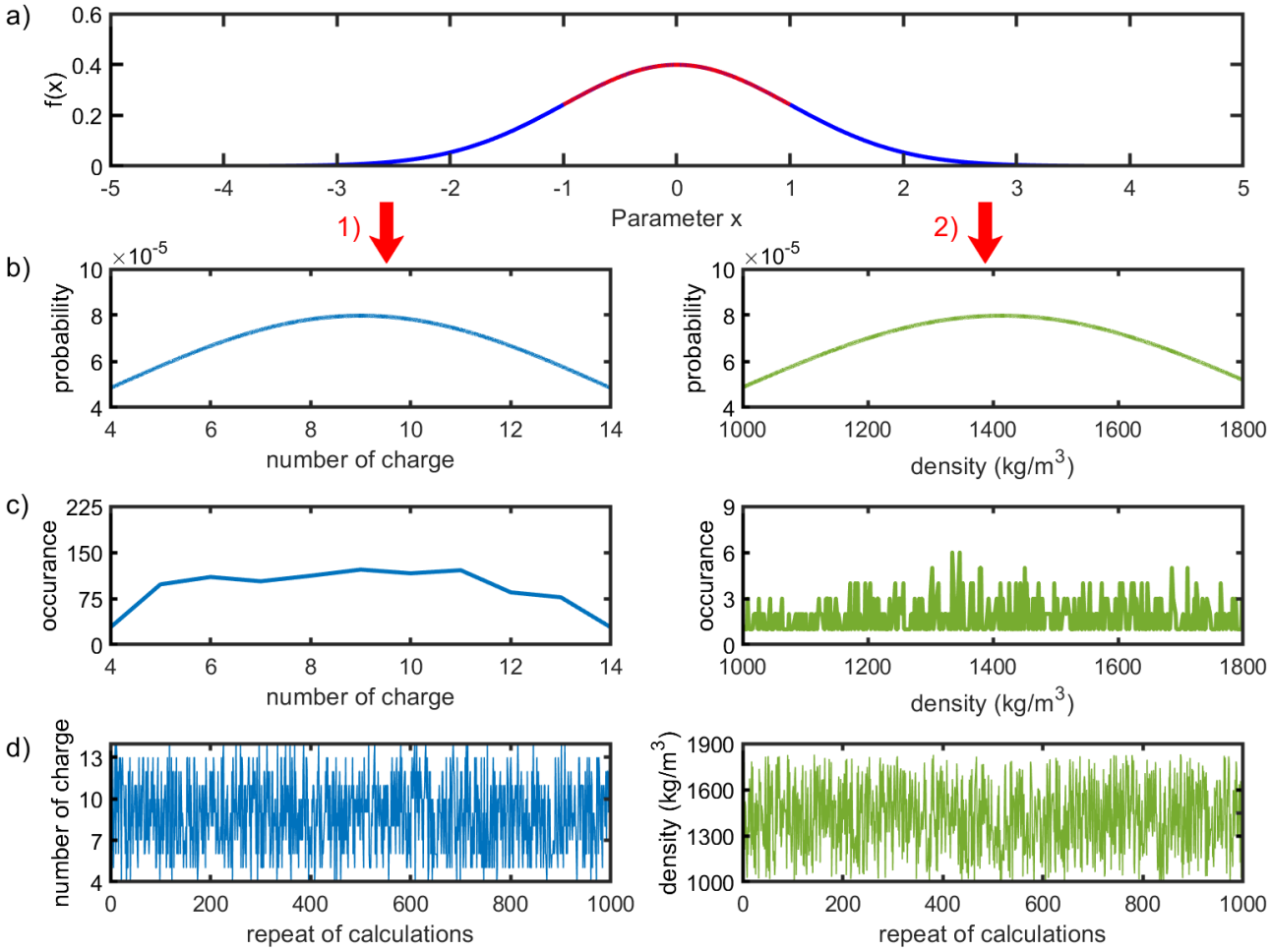

Figure S2: Validating the robustness of rate coefficients calculation. Example for procedure to randomly vary input parameters (here for number of charges and particle density). Panel a) shows the weighting scheme applied to all parameters. The calculations shown in equations (1) to (9) in the main paper are then repeated 1000 times for all experiments (Panel d). During this, all parameters that could introduce statistical and systematic errors are randomly varied. A weighting scheme towards the central value of the variations is applied according to a normal distribution (Panel b and c). The derived probability distribution is applied over a specific range that is also summarized in Table S1 (Panel 2). The resulting values for number of charges and particle density and their occurrence throughout the 1000 repeats are shown in the panels c) and d).

Table S1: Variation of different parameters that contribute to the total error of the calculated coefficients. We show the central value, as well as the variation. The parameters are weighted according to a Gaussian distribution, as shown in Figure S2.

Parameter	**Unit (Parameter)**	**Central value**	**Variation**
Smallest diameter	nm	2	± 10 %
Largest diameter	nm	10	± 50 %
$k_{loss}(d_p, t)$	s^{-1}	± 500 %	± 500 %
Number of charge (j)	-	9	± 5
Particle density (ρ)	kg m^{-3}	1413	416
AIS: $\Omega_{\pm}$, ω_j	fA	Measured Value	± 0.2
nSMPS: Ω_0	cm^{-3}	Measured Value	± 400 %

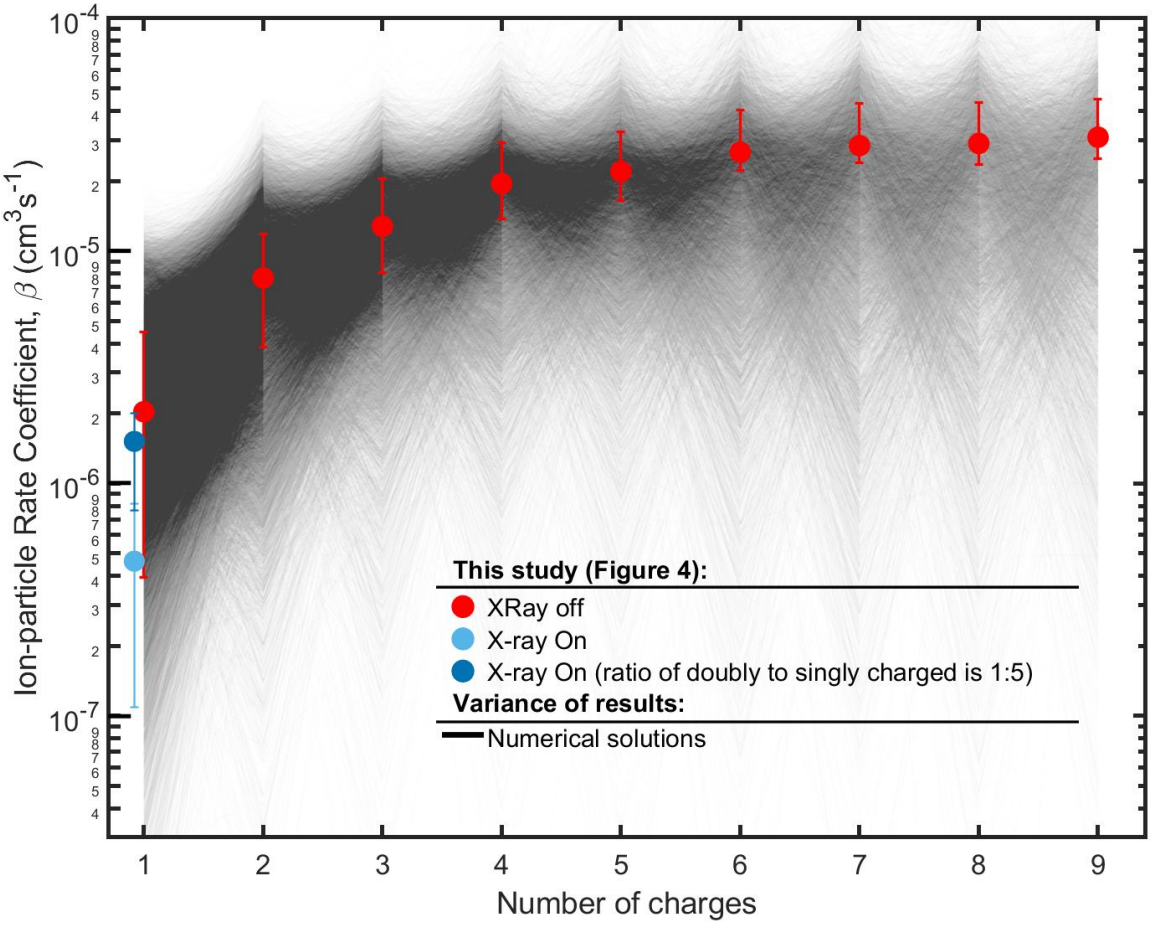

Figure S3: **Uncertainty estimate of our calculated rate coefficients overlayed with our results from Figure 4. Black lines show all numerical solutions (from all repeated calculations), with the validation scheme from Figure S2 applied.**

S2 The fraction of positively charged particles

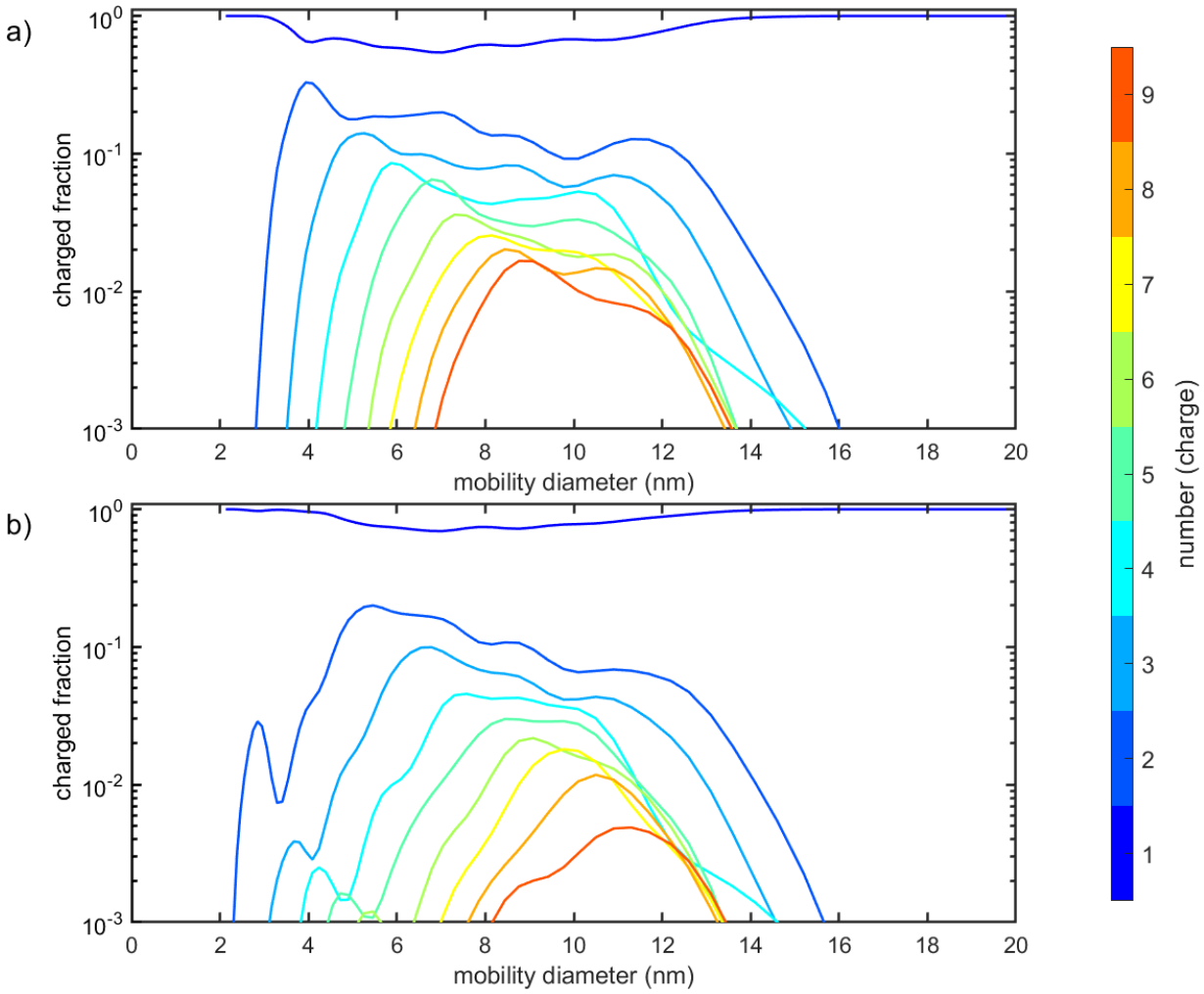

Figure S4: **An example of the charged fraction of positive particles at 0 seconds and 500 seconds in the first experiment shown in Figure 3 in the main text.**

S3 All experiments conducted

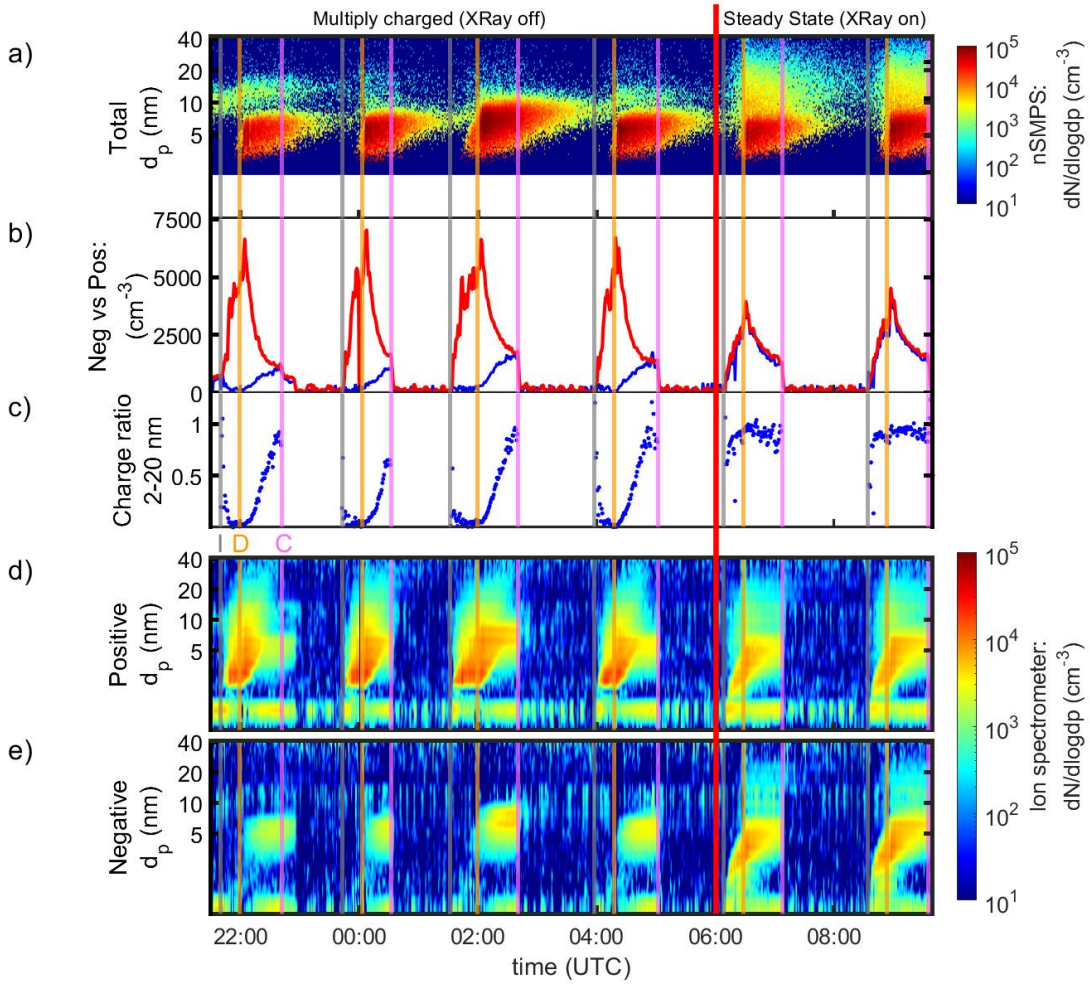

Figure S5: **All experiments conducted for this study (four with X-Ray and two without). We only show the two of each in the main text in Figure 3.**

References

Dunne, E. M., Gordon, H., Kürten, A., Almeida, J., Duplissy, J., Williamson, C., Ortega, I. K., Pringle, K. J., Adamov, A., Baltensperger, U., Barmet, P., Benduhn, F., Bianchi, F., Breitenlechner, M., Clarke, A., Curtius, J., Dommen, J., Donahue, N. M., Ehrhart, S., Flagan, R. C., Franchin, A., Guida, R., Hakala, J., Hansel, A., Heinritzi, M., Jokinen, T., Kangasluoma, J., Kirkby, J., Kulmala, M., Kupc, A., Lawler, M. J., Lehtipalo, K., Makhmutov, V., Mann, G., Mathot, S., Merikanto, J., Miettinen, P., Nenes, A., Onnela, A., Rap, A., Reddington, C. L. S., Riccobono, F., Richards, N. A. D., Rissanen, M. P., Rondo, L., Sarnela, N., Schobesberger, S., Sengupta, K., Simon, M., Sipilä, M., Smith, J. N., Stozkhov, Y., Tomé, A., Tröstl, J., Wagner, P. E., Wimmer, D., Winkler, P. M., Worsnop, D. R., and Carslaw, K. S.: Global atmospheric particle formation from CERN CLOUD measurements, Science, 354, 1119–1124, https://doi.org/10.1126/science.aaf2649, 2016.

Kangasluoma, J., Cai, R., Jiang, J., Deng, C., Stolzenburg, D., Ahonen, L. R., Chan, T., Fu, Y., Kim, C., Laurila, T. M., Zhou, Y., Dada, L., Sulo, J., Flagan, R. C., Kulmala, M., Petäjä, T., and Lehtipalo, K.: Overview of measurements and current instrumentation for 1–10 nm aerosol particle number size distributions, Journal of Aerosol Science, 148, 105584, https://doi.org/10.1016/j.jaerosci.2020.105584, 2020.

Kürten, A., Rondo, L., Ehrhart, S., and Curtius, J.: Performance of a corona ion source for measurement of sulfuric acid by chemical ionization mass spectrometry, Atmos. Meas. Tech., 4, 437–443, https://doi.org/10.5194/amt-4-437-2011, 2011.

Nieminen, T., Lehtinen, K. E. J., and Kulmala, M.: Sub-10 nm particle growth by vapor condensation – effects of vapor molecule size and particle thermal speed, Atmos. Chem. Phys., 10, 9773–9779, https://doi.org/10.5194/acp-10-9773-2010, 2010.

Vehkamäki, H., Kulmala., M., Napari, I., Lehtinen, K. E. J., Timmreck, M., Noppel, M., and Laaksonen, A.: An improved parameterization for sulfuric acid–water nucleation rates for tropospheric and stratospheric conditions, J. Geophys. Res., 107, AAC 3-1-AAC 3-10, https://doi.org/10.1029/2002JD002184, 2002.